Computers & Structures Vol. 22, No. 5, pp. 831–839, 1986
Printed in Great Britain.

0045–7949/86 $3.00 + .00

NONLINEAR ANALYSIS OF FRAMED STRUCTURES WITH A PLASTICITY MINDED BEAM ELEMENT

BERNARD ESPION
Service Génie Civil, Université Libre de Bruxelles, B-1050, Brussels, Belgium

(*Received* 29 *January* 1985)

Abstract—A general method for geometrical and material nonlinear analysis of planar framed structures is presented. The theoretical prerequisites prior to the development of a displacement type approach for a beam element in plasticity are established. The shape functions and stiffness matrix for a nine-d.o.f. beam element are evaluated. The generalised updated Lagrangian formulation is used to describe the equations of equilibrium and the predictions of a computer program are compared with examples ranging from buckling and elastica problems to experimental plasticity in steel and in reinforced concrete.

1. INTRODUCTION

Piecewise linear structures consisting of beams and columns are among the most widely used and designed. Widespread computer usage in engineering offices allows us to now take into account the nonlinear behavior of structures and to gain a better idea of the actual safety factor against failure. Moreover, in some cases, such as the stability analysis of unbraced frames, second-order computations are compulsorily prescribed by construction codes. For materials like reinforced concrete, nonlinear behavior produced by the material itself exists already for loads of the magnitude of the service loads and carefull assessment of the nonlinear material effects (for instance, tension stiffening or creep) is necessary for checking the serviceability limit states.

With the advance of computer-aided design, a growing demand thus exists for general-purpose programs of analysis of framed structures, and they have to be flexible enough to treat various materials (composite structures) and to give a fine response of the structure to various limit states (ultimate, buckling, serviceability).

Up to now, such programs were scarce. Even in large standard FEM codes, combined plasticity and large displacements are not always treated rigorously. Reinforced concrete models in such programs are generally not suitable for beam/column engineering analysis. On the other hand, office design programs are often too specialized, and their applicability is frequently restricted by theoretical assumptions and by the hypotheses regarding the physical behavior of the model.

The beam element developed here is presented in a general displacement approach but is simple enough to be used in structural engineering practice and does not suffer from the theoretical drawbacks of some of its predecessors.

2. THE SHAPE FUNCTIONS OF THE BEAM ELEMENT

The usual beam element in most codes is shown in Fig. 1 with only the six-d.o.f. (degrees of freedom) $q_1, q_2, q_3, q_4, q_5, q_6$ at the boundaries of the element. The shape functions underlying the displacement field of this element are complete polynomials of the third order for the transverse displacement v and of the first order for the longitudinal displacement u.

Let u_i be the Cartesian component of the incremental displacement of a point (x, y) in the ith direction. The standard FEM displacement approach assumes that u_i is a function of the incremental nodal displacements q_k chosen as unknowns.

$$u_i = \sum_{k=1}^{6} N_k^i q_k, \qquad u_1 = u, \qquad u_2 = v. \tag{1}$$

The generalised Navier–Bernoulli hypothesis regarding the planarity of the sections after bending states that

$$u(x, y) = u_0(x, y = 0) - y \frac{\mathrm{d}v}{\mathrm{d}x}. \tag{2}$$

When the local x-axis does not coincide with the line of the centroids† of the sections, this relationship implies that the difference between the order of the polynomials for u and v is only one, not two.

In material nonlinear behavior, it is quite clear that the centroid moves across the depth of the section during the loading process and we can conclude that the use of the traditional shape functions of the six-d.o.f. beam element would theoretically be inconsistent, in plasticity, with the most important

† The centroid of the section is the point such that $K_1 = 0$ in eqns (11), when $y = 0$ is the ordinate of the centroid.

hypothesis (and experimental evidence). This is why Blaauwendraad[1] and Aldstedt and Bergan[2] after him have introduced a seventh d.o.f., namely a tangential displacement at midlength of the beam element so that the order of the displacement field for u would be raised to the second.

Nevertheless, this solution could practically prove insufficient in some cases for the following reasons. In a far advanced material nonlinear state, plastic deformations concentrate in critical sections (plastic hinges) where the curvature varies sharply along the beam. If one wishes to use as few elements as possible to represent the whole structure, it is probable that a seven-d.o.f. element with its associated linear curvature field will only produce a rough image of the reality. Secondly, it will be seen here that taking into account the geometrical nonlinear effects and evaluating the nodal forces equivalent to the internal stresses (what is made compulsory in the iterative solution process of the nonlinear system of equilibrium equations) require precise knowledge of the stress–strain distribution in the sections of numerical integration. Through the stress–strain relationship of the materials, the stresses depend explicitly on the order of the displacement field, which is itself physically related to the load distribution acting upon the element.

The preceding remarks led us to develop the theory of a nine-d.o.f. beam element (Fig. 1), where the transverse displacement field v would be a complete polynomial of the fourth order in x, and the longitudinal displacement field u a third-order polynomial in x (the choice of the longitudinal position of the intermediate d.o.f. q_7, q_8, q_9 is arbitrary).

Such an assumed displacement field is consistent with a constant distributed transverse and tangential load and bring on a second-order curvature field which is accurate enough to represent parts of beams and columns in a material nonlinear state.

Let u and v be defined as

$$u = \alpha_0 + \alpha_1 x + \alpha_2 x^2 + \alpha_3 x^3,$$
$$v = \beta_0 + \beta_1 x + \beta_2 x^2 + \beta_3 x^3 + \beta_4 x^4 \qquad (3)$$

and suppose also that u and v are polynomial functions of the unknowns q_i:

$$\begin{Bmatrix} u \\ v \end{Bmatrix} = \begin{bmatrix} N_1^1 & N_2^1 & N_3^1 & \cdots & N_9^1 \\ N_1^2 & N_2^2 & N_3^2 & \cdots & N_9^2 \end{bmatrix} \begin{Bmatrix} q_1 \\ \vdots \\ q_9 \end{Bmatrix}. \qquad (4)$$

Identifying (3) and (4) with respect to the kinematic boundary conditions and with (2), we get the necessary shape functions

$$\xi = x/L, \qquad \eta = y/L. \qquad (5)$$

$$\begin{aligned}
N_1^1 &= (2 - 11\xi + 18\xi^2 - 9\xi^3)/2, \\
N_2^1 &= \eta(22\xi - 54\xi^2 + 32\xi^3), \\
N_3^1 &= y(8\xi - 15\xi^2 + 8\xi^3 - 1), \\
N_4^1 &= (2\xi - 9\xi^2 + 9\xi^3)/2, \\
N_5^1 &= \eta(10\xi - 42\xi^2 + 32\xi^3), \\
N_6^1 &= y(-2\xi + 9\xi^2 - 8\xi^3), \\
N_7^1 &= (18\xi - 45\xi^2 + 27\xi^3)/2, \\
N_8^1 &= \eta(-32\xi + 96\xi^2 - 64\xi^3), \\
N_9^1 &= (-9\xi + 36\xi^2 - 27\xi^3)/2,
\end{aligned}$$

$$\begin{aligned}
N_1^2 &= 0, \\
N_2^2 &= 1 - 11\xi^2 + 18\xi^3 - 8\xi^4, \\
N_3^2 &= L(\xi - 4\xi^2 + 5\xi^3 - 2\xi^4), \\
N_4^2 &= 0, \\
N_5^2 &= (-5\xi^2 + 14\xi^3 - 8\xi^4), \\
N_6^2 &= L(\xi^2 - 3\xi^3 + 2\xi^4), \\
N_7^2 &= 0, \\
N_8^2 &= 16\xi^2 - 32\xi^3 + 16\xi^4, \\
N_9^2 &= 0.
\end{aligned}$$

The development of the nine-d.o.f. beam element could sound strange to the structural engineer who knows perfectly well that the shape and order of the generalised stress distributions (i.e. bending moment, shear and normal forces) are given by statics and that only six usual kinematical quantities ($q_1, \ldots, q_6$) are necessary to completely describe the motion of the beam element. In fact, the additional d.o.f. q_7, q_8, q_9 are dummy, in the sense that, connecting no other element, they can be expressed as functions of the boundary d.o.f. and eliminated in the equations of equilibrium of the element.

Since we want to deal with structures with a relatively high slenderness ratio or with massive sec-

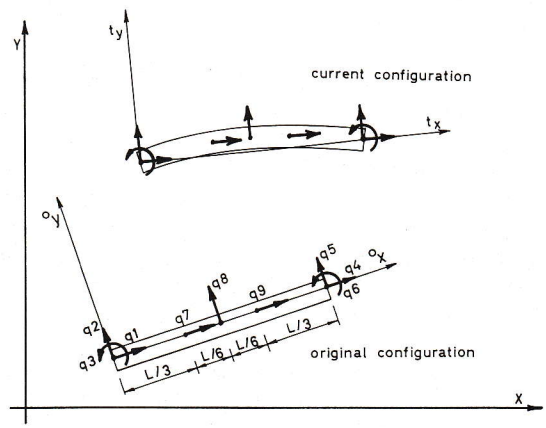

Fig. 1. The nine-d.o.f. beam element.

tions (like most reinforced concrete sections), the influence of shear deformations may be disregraded.

3. NONLINEAR INCREMENTAL FORMULATION

The general nonlinear formulation adopted here is the one developed by Bathe, called updated Lagrangian[3–5], better named approximated updated Lagrangian according to Frey[6], when dealing with small strains and oriented structures like beams, plates and shells. The reader is referred to the papers by Bathe for the notation; for the sake of brevity, we only mention that a left superscript denotes the time of the configuration (i.e. load step) in which the quantity occurs and that a left subscript denotes the time of the configuration (i.e. load step) in which the quantity is measured.

In this description, the linearised equilibrium equation, resulting from the principle of virtual displacements expressed in the last equilibrium configuration may be written as

$$\int_v {}_tC_{ijrs}\,{}_te_{rs}\,\delta\,{}_te_{ij}\,\mathrm{d}V + \int_v {}^t\sigma_{ij}\,\delta\,{}_t\eta_{ij}\,\mathrm{d}V = {}^{t+\Delta t}\mathcal{R} - \int_v {}^t\sigma_{ij}\,\delta\,{}_te_{ij}\,\mathrm{d}V, \quad (6)$$

where ${}^{t+\Delta t}\mathcal{R}$ is the total virtual work due to the external forces; ${}^t\sigma_{ij}$ are the Cartesian components of the Cauchy stress tensor; ${}_te_{ij}$ and ${}_t\eta_{ij}$ are the Cartesian components of the linear and nonlinear strain increments, respectively, and the ${}_tC_{ijrs}$ are the components of the tangent constitutive tensor relating small strain increments to the corresponding stress increments; δ represents a small virtual variation of the related variable. Using the displacement-type approach of the FEM, the continuum mechanics formulation (6) is transcribed into the following set of equilibrium equations for a single element in global Cartesian axes:

$$[{}^0\overline{R}]^{\mathrm{T}}\,[{}^t\overline{R}]^{\mathrm{T}}[{}^tK_{\mathrm{L}}]\,[{}^t\overline{R}]\,[{}^0\overline{R}]\,\{q\} + [{}^0\overline{R}]^{\mathrm{T}}\,[{}^t\overline{R}]^{\mathrm{T}}\,[{}^tK_{\mathrm{NL}}]\,[{}^t\overline{R}]\,[{}^0\overline{R}]\{q\} = \{{}^{t+\Delta t}R\} - [{}^0\overline{R}]^{\mathrm{T}}\,[{}^t\overline{R}]^{\mathrm{T}}\,\{{}^tF\}. \quad (7)$$

With $\{q\}$ the vector of incremental nodal displacements between the two equilibrium configurations t and $t + \Delta t$, $[{}^tK_{\mathrm{L}}]$ is the material incremental stiffness matrix and $[{}^tK_{\mathrm{NL}}]$ is the geometric incremental stiffness matrix; $\{{}^{t+\Delta t}R\}$ is the vector of nodal forces equivalent to applied external loads, and $\{{}^tF\}$ the vector of nodal forces equivalent to internal stresses.

Neglecting the influence of shear, the incremental stress–strain tensor resumes, in two-dimensional beams, to a simple uniaxial incremental tangent modulus, and we get

$${}^tK_{\mathrm{L}}^{ij} = \int_v E_t\,N_{i,1}^1\,N_{j,1}^1\,\mathrm{d}V, \quad (8)$$

$${}^tK_{\mathrm{NL}}^{ij} = \int_v {}^t\sigma_x\,N_{i,1}^2\,N_{j,1}^2\,\mathrm{d}V, \quad (9)$$

$${}^tF_i = \int_v {}^t\sigma_x\,N_{i,1}^1\,\mathrm{d}V, \quad (10)$$

where $N_{i,1}^j$ stands for $\mathrm{d}N_i^j/\mathrm{d}x$. $[{}^0\overline{R}]$ and $[{}^t\overline{R}]$ are the transformation matrices between the initial configuration and global coordinates axes and between the current and original configurations, respectively.

The formulation adopted herein is a general displacement-type approach with the usual beam assumptions. Since the additional d.o.f. q_7, q_8, q_9 may be eliminated by static condensation in eqn (7), it is now quite clear that the only purpose of introducing these kinematic dummy parameters is to evaluate with a reasonable accuracy the stiffness matrices (8), (9) and the load vector (10) by taking into account some physical insights regarding the spread of plasticity across the sections and along the element.

A semi-inverse hybrid type formulation has been adopted by Backlund[7], who first assumes the distribution of bending moment and normal force along the element, then evaluates the (material) flexibility matrix and takes it inverse to obtain the elementary stiffness matrix. The hypothesis there lies in the choice of the order of the bending moment and normal force fields.

4. ELASTIC STIFFNESS MATRIX

The stiffness $[{}^tK_{\mathrm{NL}}]$ (9) and the load vector $\{{}^tF\}$ (10) will always be evaluated numerically; on the other hand, computer time saving could be achieved in material linear analysis when using the analytical form of the material stiffness matrix $[{}^tK_{\mathrm{L}}]$ (8) (for a prismatic beam element). Let K_0, K_1 and K_2 be, respectively, the zero-, first- and second-order moments of the elastic weights $E\,\mathrm{d}\Omega$:

$$K_0 = \int_\Omega E\,\mathrm{d}\Omega, \qquad K_1 = \int_\Omega Ey\,\mathrm{d}\Omega, \qquad K_2 = \int_\Omega Ey^2\,\mathrm{d}\Omega. \quad (11)$$

Then, differentiating the shape functions (5) with respect to x according to the needs of (8) and in-

tegrating analytically, we obtain

$$\begin{bmatrix}
\frac{37}{10}\frac{K_0}{L} & -\frac{117}{10}\frac{K_1}{L^2} & -\frac{101}{20}\frac{K_1}{L} & -\frac{13}{40}\frac{K_0}{L} & -\frac{27}{10}\frac{K_1}{L^2} & \frac{11}{20}\frac{K_1}{L} & -\frac{189}{40}\frac{K_0}{L} & \frac{72}{5}\frac{K_1}{L^2} & \frac{27}{20}\frac{K_0}{L} \\
 & \frac{316}{5}\frac{K_2}{L^3} & \frac{94}{5}\frac{K_2}{L^2} & \frac{27}{10}\frac{K_1}{L^2} & \frac{196}{5}\frac{K_2}{L^3} & -\frac{34}{5}\frac{K_2}{L^2} & \frac{261}{10}\frac{K_1}{L^2} & -\frac{512}{5}\frac{K_2}{L^3} & -\frac{171}{10}\frac{K_1}{L^2} \\
 & & \frac{36}{5}\frac{K_2}{L} & \frac{11}{20}\frac{K_1}{L} & \frac{34}{5}\frac{K_2}{L^2} & -\frac{6}{5}\frac{K_2}{L} & \frac{153}{20}\frac{K_1}{L} & -\frac{128}{5}\frac{K_2}{L^2} & -\frac{63}{20}\frac{K_1}{L} \\
 & & & \frac{37}{10}\frac{K_0}{L} & \frac{117}{10}\frac{K_1}{L^2} & -\frac{101}{20}\frac{K_1}{L} & \frac{27}{20}\frac{K_0}{L} & -\frac{72}{5}\frac{K_1}{L^2} & -\frac{189}{40}\frac{K_0}{L} \\
 & & & & \frac{316}{5}\frac{K_2}{L^3} & -\frac{94}{5}\frac{K_2}{L^2} & \frac{171}{10}\frac{K_1}{L^2} & -\frac{512}{5}\frac{K_2}{L^3} & -\frac{261}{10}\frac{K_1}{L^2} \\
 & & & & & \frac{36}{5}\frac{K_2}{L} & -\frac{63}{20}\frac{K_1}{L} & \frac{128}{5}\frac{K_2}{L^2} & \frac{153}{20}\frac{K_1}{L} \\
 & & & & & & \frac{54}{5}\frac{K_0}{L} & -\frac{216}{5}\frac{K_1}{L^2} & -\frac{297}{40}\frac{K_0}{L} \\
 & & & & & & & \frac{1024}{5}\frac{K_2}{L^3} & \frac{216}{5}\frac{K_1}{L^2} \\
 & & & & & & & & \frac{54}{5}\frac{K_0}{L}
\end{bmatrix} \cdot \begin{Bmatrix} q_1 \\ q_2 \\ q_3 \\ q_4 \\ q_5 \\ q_6 \\ q_7 \\ q_8 \\ q_9 \end{Bmatrix} = \begin{Bmatrix} p_x\frac{L}{8} \\ \frac{7}{30}p_yL + sp_x \\ \frac{p_yL^2}{60} \\ p_x\frac{L}{8} \\ \frac{7}{30}p_yL - sp_x \\ -\frac{p_yL^2}{60} \\ \frac{3}{8}p_xL \\ \frac{16}{30}p_yL \\ \frac{3}{8}p_xL \end{Bmatrix}. \quad (12)$$

The right side vector of the system (12) contains the elementary nodal forces equivalent to constant distributed transversal and tangential loads acting upon the element at the level s from the local x-axis. From the last three equations of (12), we can have the values of q_7, q_8, q_9 as functions of the other unknowns, the load, the geometry and the elastic properties of the element.

$$q_7 = \frac{p_xL^2}{9K_0} + \frac{1}{162}\frac{K_1L^3}{(K_0K_2 - K_1^2)}p_y + \frac{2}{3}q_1 + \frac{1}{3}q_4 - \frac{4}{3}\frac{K_1}{K_0L}q_2 - \frac{2}{3}\frac{K_1}{K_0}q_3 + \frac{4}{3}\frac{K_1}{K_0L}q_5 - \frac{2}{3}\frac{K_1}{K_0}q_6, \quad (13.1)$$

$$q_8 = \frac{p_yL^4}{384}\left(\frac{K_0}{K_0K_2 - K_1^2}\right) + \frac{q_2 + q_5}{2} + \frac{q_3 - q_6}{8}L, \quad (13.2)$$

$$q_9 = \frac{p_xL^2}{9K_0} - \frac{1}{162}\frac{K_1L^3}{(K_0K_2 - K_1^2)}p_y + \frac{1}{3}q_1 + \frac{2}{3}q_4 - \frac{4}{3}\frac{K_1}{K_0L}q_2 - \frac{2}{3}\frac{K_1}{K_0}q_3 + \frac{4}{3}\frac{K_1}{K_0L}q_5 - \frac{2}{3}\frac{K_1}{K_0}q_6. \quad (13.3)$$

Eliminating (13) with the first six equations of (12) leads to the reduced 6×6 system of equilibrium equations

$$\begin{bmatrix}
\frac{K_0}{L} & 0 & -\frac{K_1}{L} & -\frac{K_0}{L} & 0 & \frac{K_1}{L} \\
 & \frac{12}{L^3}\frac{K_0K_2 - K_1^2}{K_0} & \frac{6}{L^2}\frac{K_0K_2 - K_1^2}{K_0} & 0 & -\frac{12}{L^3}\frac{K_0K_2 - K_1^2}{K_0} & \frac{6}{L^2}\frac{K_0K_2 - K_1^2}{K_0} \\
 & & \frac{1}{L}\frac{4K_0K_2 - 3K_1^2}{K_0} & \frac{K_1}{L} & -\frac{6}{L^2}\frac{K_0K_2 - K_1^2}{K_0} & \frac{1}{L}\frac{2K_0K_2 - 3K_1^2}{K_0} \\
 & & & \frac{K_0}{L} & 0 & -\frac{K_1}{L} \\
 & & & & \frac{12}{L^3}\frac{K_0K_2 - K_1^2}{K_0} & -\frac{6}{L^2}\frac{K_0K_2 - K_1^2}{K_0} \\
 & & & & & \frac{1}{L}\frac{4K_0K_2 - 3K_1^2}{K_0}
\end{bmatrix} \cdot \begin{Bmatrix} q_1 \\ q_2 \\ q_3 \\ q_4 \\ q_5 \\ q_6 \end{Bmatrix} = \begin{Bmatrix} p_x\frac{L}{2} \\ p_x\left(s - \frac{K_1}{K_0}\right) + p_y\frac{L}{2} \\ p_y\frac{L^2}{12} - p_x\frac{L}{2}\frac{K_1}{K_0} \\ p_x\frac{L}{2} \\ p_x\left(\frac{K_1}{K_0} - s\right) + p_y\frac{L}{2} \\ -p_y\frac{L^2}{12} - p_x\frac{L}{2}\frac{K_1}{K_0} \end{Bmatrix}. \quad (14)$$

To the best of our knowledge and despite its great practical importance, the stiffness matrix (14) has never been published. Assuming $K_0 = E\Omega$, $K_1 = 0$, $K_2 = EI$, system (14) is strictly identical to the stiffness matrix of the beam element found in any structural textbook. System (14) shows the exact additional terms required by the analysis when the local x-axis no longer coincides with the centroid of the section (i.e. $K_1 \neq 0$). This circumstance is often met in practice—for instance, to represent beam-to-column or beam-to-beam connections or when studying composite girders and beams without computing *a priori* the position of the centroid of the section.

5. COMPUTER PROGRAM ORGANISATION

Assembly of the elementary equations (7) into a global set of equilibrium equations for the whole structure requires the step-by-step solution of a nonlinear system of equations. A purely tangential Newton–Raphson algorithm is used for the examples presented in this paper:

$$[{}^0\overline{R}]^T[{}^{t+\Delta t}\overline{R}^{(k-1)}]^T[{}^{t+\Delta t}K_L^{(k-1)} + {}^{t+\Delta t}K_{NL}^{(k-1)}] \times [{}^{t+\Delta t}\overline{R}^{(k-1)}][{}^0\overline{R}]\{\Delta Q^{(k)}\} = \{{}^{t+\Delta t}R\} - [{}^0\overline{R}]^T[{}^{t+\Delta t}\overline{R}^{(k-1)}]^T\{{}^{t+\Delta t}F^{(k-1)}\}, \quad (15.1)$$

$${}^{t+\Delta t}Q^{(k)} = {}^{t+\Delta t}Q^{(k-1)} + \Delta Q^{(k)}, \quad (15.2)$$

$${}^{t+\Delta t}Q^{(0)} = {}^tQ. \quad (15.3)$$

Iterations are performed until the nodal forces

equivalent to external loads are equilibrated by nodal forces equivalent to internal stresses.

In the first-order analysis, the geometric stiffness matrix disappears in (15), and the $[{}^{t+\Delta t}\overline{R}]$ transformation matrix vanishes into a unity matrix.

It must be pointed out that in a nonlinear analysis, static condensation of the 9×9 stiffness matrix into a reduced 6×6 is probably not economical since the costs saved in the memory by the reduced size of the system is offset by the enormous number of input/output operations on disks where eliminated equations like (13) have to be stored.

Newton–Cotes quadrature has been used to numerically evaluate the stiffness matrices and load vectors. It has been found that a four-points formula gives accurate results for integration along the x-axis. In material nonlinear analysis, a greater number of points is necessary to compute the sectional quantities K_0, K_1, K_2 and the normal force and bending moment (generally two or three layers, depending on the geometry of the section, and seven points on each layer).

Various stress–strain relationships—linear, bilinear, trilinear—for cold worked steel and for concrete have been incorporated and tested into the computer program. This program may be run either in nonlinear elastic analysis from a material point of view or in hypoelastic analysis (full plasticity with stresses depending on the history of the loading process).

In the following examples, original units have been kept for the clarity of comparison.

6. EXAMPLES

6.1 *Clamped arch under normal pressure*

The first tests of the computer program were made on problems where the nonlinearity is only geometric and for which theoretical solutions are known. For a circular clamped arch under increasing normal pressure like the one in Fig. 2, we have a solution given by Schreyer and Masur[8]. It is well known that, according to the shallowness and flexural rigidity of the arch, this type of structure may buckle (symmetrically or not) or not buckle. For the problem presented here, the behavior of the arch does not exhibit the "snap-through" phenomenon. The load-deflection (at midspan) curve is given in Fig. 2. Five straight elements were used to represent half of the arch.

6.2 *Cantilever beam under uniformly distributed vertical load*

In the first example, displacements were large but could still be termed as moderate with respect to the depth of the section. In this second example (Fig. 3)—an elastica problem—displacements and rotations are large regarding not only the span but also the depth. A first, semitheoretical, solution of this problem was given by Rohde[9]. A better theoretical one was produced later by Holden[10] against which our values are compared. Numerical analysis of this problem has been given by several authors, among them Bathe[5] and Yang[11]. Five elements were used to represent the whole structure.

6.3 *Simply supported beam in elasto–plastic flexure*

The third example deals with a problem in which nonlinearity is only produced by the behavior of the material.

The simply supported beam in Fig. 4 has a rectangular cross section, and its material is elastic–perfectly plastic. The load is a uniformly distributed vertical load. According to the shape factor of the rectangular section (1.5), a nonlinear behavior is expected in the last third of the loading range before reaching the perfectly plastic failure load. The theoretical solution of this well-known problem was given by Prager and Hodge[12]. Five elements of unequal length were used to represent half of the

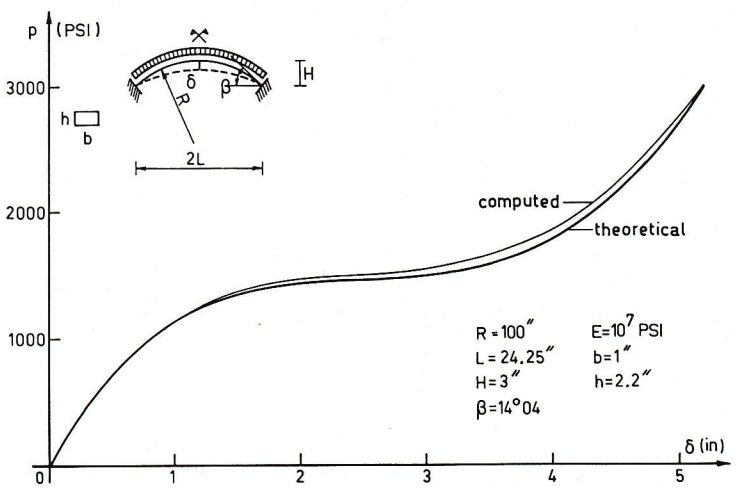

Fig. 2. Clamped arch under normal pressure.

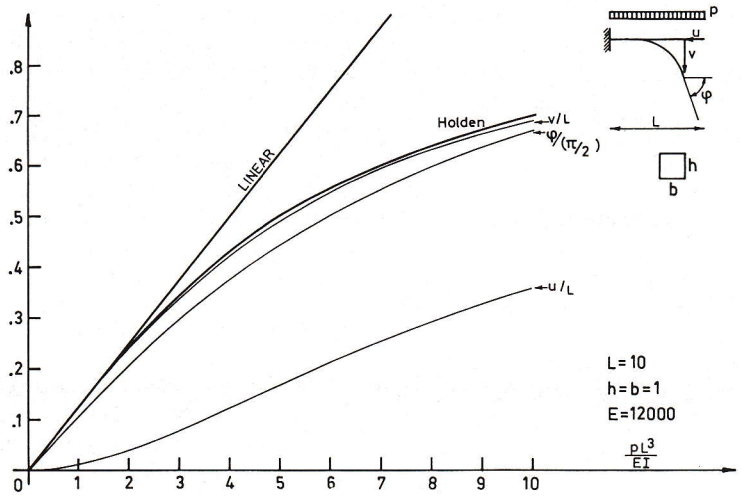

Fig. 3. Cantilever beam under uniformly distributed vertical load.

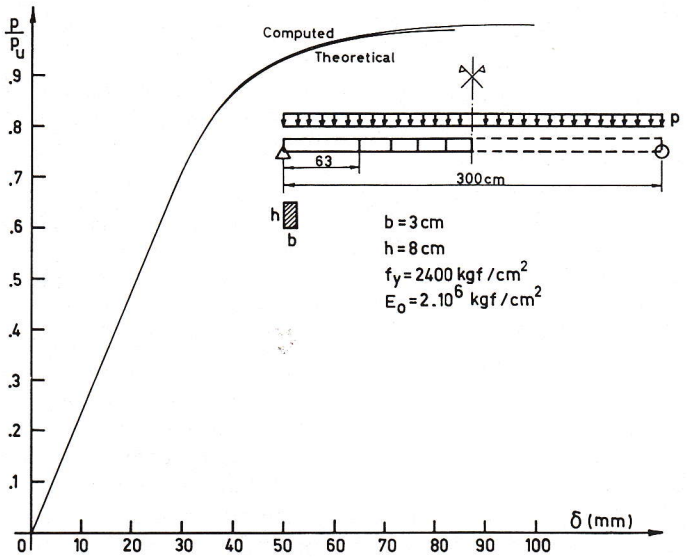

Fig. 4. Simply supported beam in elasto–plastic flexure.

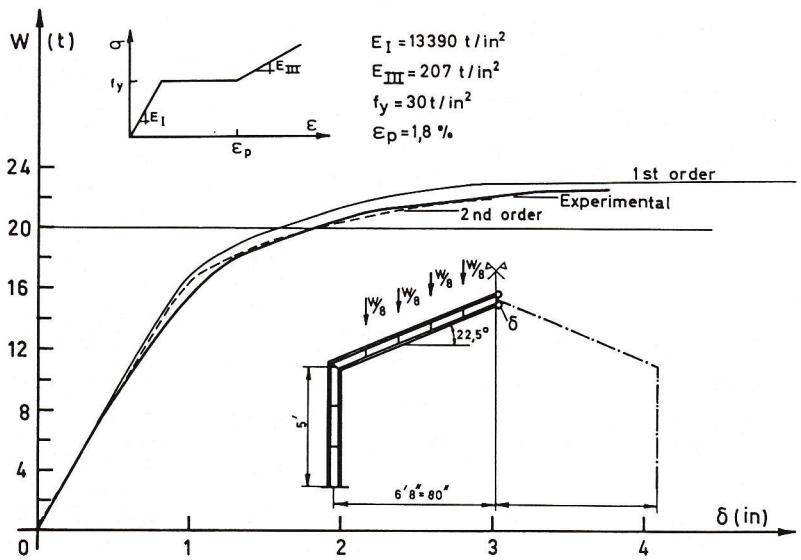

Fig. 5. Fixed-based, pitched-roof portal frame.

structure, and each element was three-layered. The load was applied in one shot up to the onset of yielding and then added in small increments up to failure. Figure 4 gives the load-deflection curve of the midspan section.

In these three first examples it should be noted that the load was uniformly distributed in local or global axes. The nine-d.o.f. beam element with its high-order shape functions chosen (among other reasons) for such cases has shown excellent agreement with the theoretical solutions. The last three examples are comparisons between experimental and computed values since, after all, physical evidence is the only matching test for a mathematical model.

6.4 *Fixed-based, pitched-roof portal frame*

The frame represented in Fig. 5 is the three-times statically indeterminate frame FB-1 tested by Horne and Chin[13]. The frame was of uniform section throughout and fabricated from 5″ × 3″ × 9 lb RSJ in high yield stress steel BS968. The characteristics of the test are precisely known, especially the true stress–strain relationship. Vertical deflection of the apex is given as a function of the total external load in Fig. 5. Two types of analysis were run: a first-order displacement analysis assuming an elastic–perfectly plastic material behavior and a large displacement-type analysis with a trilinear stress–strain relationship. It can be seen in Fig. 5 that the experimental failure load lies between the failure loads predicted by the two different analyses.

The same trend has been observed by us with nearly all the frames tested in the fifties and sixties, whose results may be found in the literature, when simple limit design received its experimental validation. If the results of the computer program prove right, this means firstly, that the actual bending moment developed in the plastic hinges could be greater than the fully plastic moment (horizontal line on Fig. 5 indicates when strain hardening begins) and secondly that this beneficial resistance is superseded by the second-order effects which produce a global stability failure. This not well-known interpretation has already been suggested by some experimentalists.

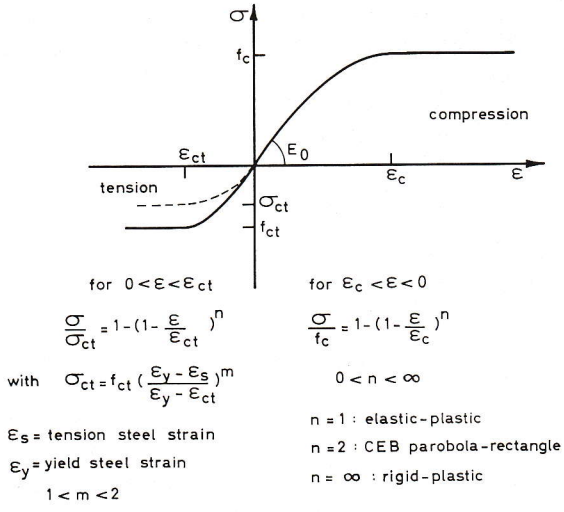

Fig. 6. Stress–strain relationship for concrete.

6.5 *Continuous reinforced concrete beam*

The last two examples are reinforced concrete structures. The stress–strain relationship of concrete has first to be defined (Fig. 6). A very interesting law has been proposed by Quast[14, 15]. The unique feature of this law (slightly modified by us) is the tension part of the relationship where the actual tensile strength of concrete is related to the tension steel strain. This fictitious stress–strain curve is used to represent the so-called tension stiffening effect and has proved extremely accurate when compared with experimental values of moment–curvature relationships of reinforced and prestressed concrete sections[14]. The compression part of this law is somewhat more conventional and the material failure occurs when the compressive concrete strain becomes greater than a prescribed value or when the tension steel is exhausted.

The reinforced concrete three-span continuous beam represented in Fig. 7 is the CP-1 beam tested by Macchi[16]. In Fig. 7, the outer support reactions values are plotted against the midspan load. The following material properties were used:

for steel (trilinear, strain hardening):

f_y: 4940 kgf/cm^2,
ϵ_p: 1.65% (when strain hardening begins),
E_I: 2,000,000 kgf/cm^2,
E_{II}: 10,000 kgf/cm^2,
E_{III}: 50,000 kgf/cm^2;

for concrete:

f_c: 400 kgf/cm^2,
ϵ_c: 2.2×10^{-3}
E_0: 350,000 kgf/cm^2,
ϵ_{ct}: 0 and 80×10^{-6},
m = 2.

The negative values of the reactions are caused by the stresses produced by the dead weight of the beam (which are not negligible). This test is an historically important one. It was especially designed to show that redistribution of bending moments in reinforced concrete occurs already in the cracked stage (importance of tension stiffening) and that simple limit analysis without check of compatibility conditions is inadequate in the analysis of statically indeterminate reinforced concrete structures since, in the present case, material failure occurs in the midspan section before the full development of the plastic moment in the support sections. Both aspects were found in our analysis (predicted concrete and steel strains in the central section for the

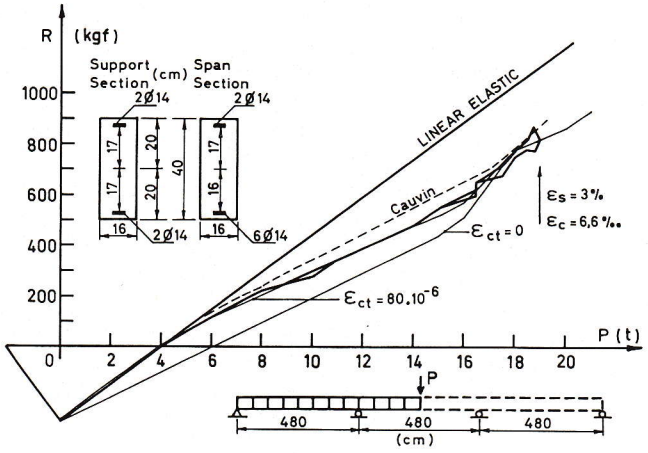

Fig. 7. Continuous reinforced concrete beam.

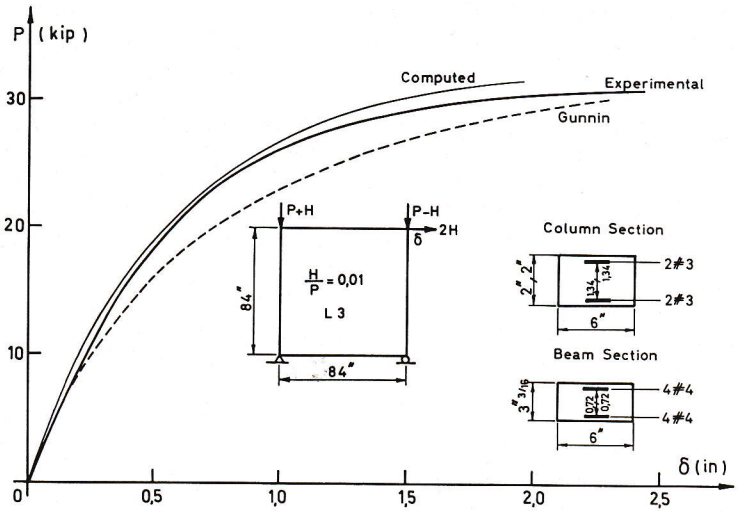

Fig. 8. Unbraced reinforced concrete frame.

experimental failure load are indicated in Fig. 7). The dashed line in Fig. 7 represents a computed solution given by Cauvin[17].

6.6 *Unbraced reinforced concrete frame*

Example 6.5 did not require a second-order analysis. In this sixth and last example, a combined geometrical and material nonlinear analysis is performed. In Fig. 8, the computational results of the column load–horizontal deflection curve are plotted together with the experimental values of the reinforced concrete frame L3 tested by Fergusson and Breen[18]. Sixteen elements of equal length were used to represent the whole structure. Material properties were

for steel (elasto–plastic):
#3 f_y = 56,400 psi,
#4 f_y = 58,500 psi,
$E = 29.3 \times 10^6$ psi,

for concrete:
f_c = 3200 psi,
$E = 3259 \times 10^3$ psi,
$\epsilon_c = 2 \times 10^{-3}$,
$\epsilon_{ct} = 0$.

A particular aspect of this test is the important amount of axial load acting on the columns, which inevitably produces a stability failure. This was perfectly found in our computer analysis. Another computed solution given by Gunnin *et al.*[19], using a generalised Ramberg–Osgood-type formulation to describe the moment–curvature relationship of a reinforced concrete beam element, is also plotted.

The somewhat less satisfactory solutions obtained by Cauvin in Example 6.5 and by Gunnin *et al.* in Example 6.6 may be attributed to the use of a simpler element and general approach than those presented in this paper.

7. CONCLUSION

The nine-d.o.f. beam element, when used in linear and nonlinear problems, has shown excellent agreement with theoretical and experimental solutions. It is generally difficult to compare the precision and the efficiency of an element with another, since frequently the authors do not give some

important characteristics of their analysis, i.e. number of elements, number of integration points. On the other hand, computer effectiveness is highly dependent on solution strategy (algorithm) and program management. This is why we would not say that simpler elements or formulations for combined nonlinear analyses could not produce good results too.

But the fine accuracy properties of this element and the general formulation adopted in this paper allow us to now take easily into account other kinds of nonlinear behavior, and, for instance, the development of a time-dependent model for reinforced concrete is currently in progress.

REFERENCES

1. J. Blaauwendraad, Realistic analysis of reinforced concrete framed structures. *Heron* **18**(4), (1972).
2. E. Aldstedt and P. G. Bergan, Non linear time-dependent concrete frame analysis. *J. Struct. Div. ASCE* **104,** 1077–1092 (1978).
3. K. J. Bathe and S. Bolourchi, Large displacement analysis of three-dimensional beam structures. *Int. J. Numer. Meth. Engng* **14,** 961–986 (1979).
4. K. J. Bathe, *Finite Element Procedures in Engineering Analysis*. Prentice-Hall, Englewood Cliffs, N.J. (1982).
5. K. J. Bathe and H. Ozdemir, Elastic–plastic large deformation static and dynamic analysis. *Comput. Struct.* **6,** 81–92 (1976).
6. F. Frey, *L'analyse statique non linéaire des structures par la méthode des eléments finis et son application à la construction métallique*, Ph.D thesis, Université de Liège (1978).
7. J. Backlund, Large deflection analysis of elasto–plastic beams and frames. *Int. J. Mech. Sci.* **18,** 269–277 (1976).
8. H. L. Schreyer and E. F. Masur, Buckling of shallow arches. *J. Struct. Div. ASCE* **92,** 1–19 (1966).
9. F. V. Rohde, Large deflections of a cantilever beam with uniformly distributed load. *Q. Appl. Math.* **11,** 337–338 (1953).
10. J. T. Holden, On the non linear deflections of thin beams. *Int. J. Solids Struct.* **8,** 1051–1055 (1972).
11. T. Y. Yang, Matrix displacement solution to elastica problems of beams and frames. *Int. J. Solids Struct.* **9,** 829–842 (1973).
12. W. Prager and P. G. Hodge, *Theory of Perfectly Plastic Solids*. John Wiley, New York (1951).
13. R. Horne and M. W. Chin, Full scale tests on portal frames of high tensile steel. *British Welding J.* **14,** 415–426 (1967).
14. U. Quast, *Rechenansätze in Form einer Spannungsdehnungsbeziehung für das Mitwirken des Betons in der gerissenen Zugzone von Stahlbetonquerschnitten*, Bericht aus dem Institut für Baustoffe, Massivbau und Brandschutz der T.U. Braunschweig (1980).
15. U. Quast, Zur Mitwirkung des Betons in der Zugzone, *Beton Stahlbetonb.* **76,** 247–250 (1981).
16. G. Macchi, Elastic distribution of moments on continuous beams. *Flexural Mechanics of Reinforced Concrete*, American Concrete Institute Special Publication SP-12, Detroit, MI, pp. 237–257 (1964).
17. A. Cauvin, Analisi non lineare di telai piani in cemento armato. *Giornale del Genio Civile* 47–66 (1978).
18. P. M. Fergusson and J. E. Breen, Investigation of the long concrete column in a frame subjected to lateral loads. *Symp. on Reinforced Concrete Columns*, American Concrete Institute Special Publication SP-13, Detroit, MI, pp. 75–119 (1966).
19. B. L. Gunnin, F. N. Rad and R. W. Furlong, A general non linear analysis of concrete structures and comparison with frame tests. *Comput. Struct.* **7,** 257–265 (1977).